

Large Velocity Gradients in the Tidal Tails of the Interacting Galaxy AM 1353–272 (“The Dentist’s Chair”) ¹

Peter M. Weilbacher², Uta Fritze-v. Alvensleben², Pierre-Alain Duc³, Klaus J. Fricke²

ABSTRACT

We present VLT observations of the interacting system AM 1353–272. Using the FORS2 instrument, we studied the kinematics of the ionized gas along its prominent tidal tails and discovered strikingly large velocity gradients associated with seven luminous tidal knots. These kinematical structures cannot be caused by streaming motion and most likely do not result from projection effects. More probably, instabilities in the tidal tails have led to the formation of kinematically decoupled objects which could be the progenitors of self-gravitating Tidal Dwarf Galaxies.

Subject headings: Galaxies: interactions – Galaxies: formation – Galaxies: kinematics and dynamics – Galaxies: individual (AM 1353-272)

1. Introduction

Interactions among disk galaxies are observed to produce tidal tails of sometimes impressive lengths containing stars and HI in varying proportions. While tidal tails of interacting galaxies have been analyzed in dynamical simulations of interactions to assess their use to probe the form of the dark matter potential (e.g. Springel & White 1999), the detailed kinematics of structures within the tidal tails have not received much attention. Both in deep spectroscopic observations (Duc et al. 2000) and high resolution dynamical simulations (Barnes & Hernquist 1992), condensations are observed to form in tidal tails, the nature and fate of which are not yet fully understood.

At a distance of 159 Mpc (computed with $H_0 = 75 \text{ km s}^{-1} \text{ Mpc}^{-1}$) the interacting system AM 1353–272, nicknamed the “The Dentist’s Chair” for its peculiar morphology, consists of three apparent components (see Fig. 1):

‘A’, a disturbed galaxy with two ~ 40 kpc long tidal tails (also cataloged as ESO 510-G 020G and IRAS F13533-2721), a disturbed edge-on disk galaxy ‘B’, and an elliptical ‘C’ (see Weilbacher et al. 2000). While ‘A’ and ‘B’ are a physical pair with a central velocity difference of only $\sim 150 \text{ km s}^{-1}$, ‘C’ has a heliocentric velocity of 14750 km s^{-1} , and is therefore located 38 Mpc behind the interacting pair. The tidal tails of AM 1353–272 A host several blue knots with luminosities of dwarf galaxies. From their location and colors, they were identified by Weilbacher et al. (2000) as Tidal Dwarf Galaxy (TDG) candidates.

In this letter, we present the first evidence from deep optical spectroscopy with the VLT that some dense structures in the tidal tails are kinematically decoupled from the overall motion of the tails. Forthcoming instruments on large telescopes — e.g. high resolution integral field spectrographs — will be very well suited to investigate further the specific dynamics in the tidal tails of AM 1353–272 A.

2. Observations and data reduction

We have obtained multi-object spectroscopic data of a field centered on the system AM 1353–272

¹Based on observations collected at the European Southern Observatory, La Silla, Chile (ESO No 67.B-0049).

²Universitäts-Sternwarte, Geismarlandstraße 11, 37083 Göttingen, Germany, {weilbach,ufritze}@uni-sw.gwdg.de

³CNRS URA 2052 and CEA, DSM, DAPNIA, Service d’Astrophysique, Centre d’Etudes de Saclay, 91191 Gif-sur-Yvette Cedex, France, paduc@cea.fr

with the FORS2 instrument at the 4th VLT telescope “Yepun”. Service mode observations were carried out in the night 13/14th of August 2001 under photometric conditions. Several spectroscopic standards were observed. The total exposure time of 3210s was split into three individual exposures of 1070s to ease cosmic ray cleaning. The seeing of $1''.0$ is well sampled by an instrumental scale of $0''.2 \text{ px}^{-1}$. The grism 600B+22 was used, giving a wavelength coverage of $3450 \dots 5900 \text{ \AA}$ and a spectral resolution of 5.7 \AA (1.2 \AA per pixel) for a central slit of $1''$ width. We created a mask for the mask exchange unit (MXU) of the FORS2 instrument with curved and tilted slits to cover the tails of AM 1353–272 A and several surrounding galaxies in one setup (see Fig. 1).

The data reduction followed standard recipes, for which we used our own IRAF task `mosx` (Weilbacher et al. 2002). Special care was taken to correct the curvature of the 2D spectra of the curved slits: a proper wavelength calibration was carried out at each position along the slits, using a reference HeHgCd frame observed through the same mask as the science frames. The typical accuracy for each column is 0.04 \AA RMS. A 4th order polynomial fit was then performed for each slit to determine the final wavelength solution and compute the parameters of the curvature correction. All these tasks were performed using the standard tools in the IRAF package `longslit`. The result of this procedure is presented in Fig. 2: the original, uncorrected 2D spectrum is compared with the spectrum after the correction.

After subtracting the sky background, we used the brightest emission lines from the slits along the tidal tails to derive the velocity profiles with an IRAF script based on the `fitprofs` procedure. As a check, the same velocity fit was carried out with the nearest lines in the wavelength calibration spectrum. The 1σ differences from zero velocity in this control fit are below 1 km s^{-1} . The *relative systematic* errors in the final velocity profiles should be of the order of 1 km s^{-1} while the errors for single points are typically 15 km s^{-1} .

3. Results

Fig. 3 presents the velocity distribution of the ionized gas along the two tails of AM 1353–272.

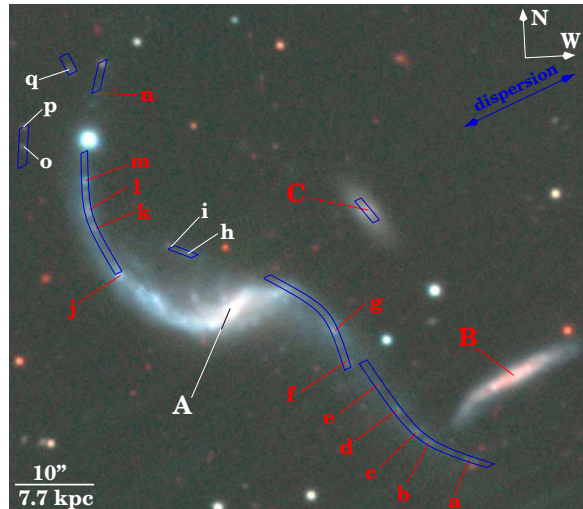


Fig. 1.— Finding chart of AM 1353–272. Original B -band image from NTT-SUSI (Weilbacher et al. 2000) in logarithmic scale. (Electronic edition: Composite $B+V+NIR$ “true” color image from NTT-SUSI and SOFI (Weilbacher et al. 2000, Weilbacher et al. in prep.).) The field of view is $\sim 2' \times 2'$. Black labels (red labels in electronic edition) mark objects with measured redshift.

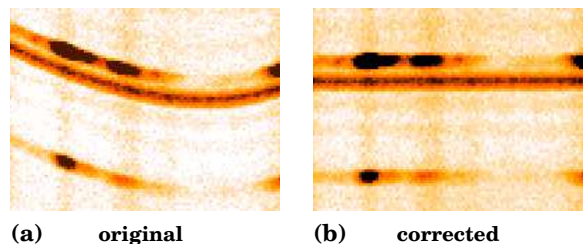


Fig. 2.— Slit curvature correction. As an example, we show part of a 2D spectrum with the emission lines $[\text{O III}]5007, 4959$ emitted by the knots ‘j’ to ‘m’. Between these object lines, a skyline is visible which allows to judge the quality of the correction.

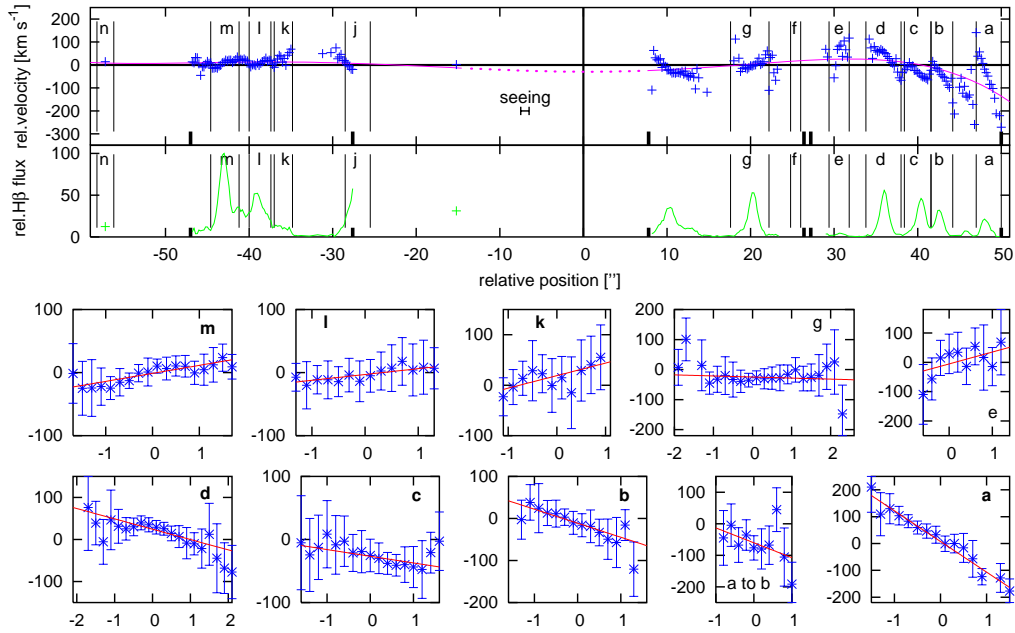


Fig. 3.— Velocities along AM 1353–272 A. **Top:** velocity field relative to a zeropoint of 11935 km s^{-1} along the ridge of the galaxy from the northern (left) to the southwestern (right) tip of the tidal tail. The seeing of $1''.0$ is indicated. The lower part shows the $\text{H}\beta$ flux in relative units on the same spatial scale. The size of each knot is marked with vertical lines. Bold marks on the position axis indicate the ends of the curved slits. A 5th order fit to the overall velocity profile is shown. **Bottom:** the extracted residual velocity field of each knot after correction for tidal motion, plotted as relative position [″] vs. relative velocity [km s^{-1}]. Lines show a linear fit.

The velocities indicated on the top of Fig. 3 are relative to the interpolated central velocity $V_A = 11935 \text{ km s}^{-1}$ of AM 1353–272 A. The relative H β flux and hence distribution of the H II regions along the tails, is shown below: it may be used to infer the S/N ratio of the emission lines used to derive the velocities. Vertical lines mark the individual optical knots studied by Weilbacher et al. (2000). Note that nearly all of them are sites of active star formation, as predicted by a comparison of photometric starburst models with optical broad band colors.

At first glance, it seems as if there are velocity gradients within the knots and sudden jumps in velocity between them. To further analyze the step-like shape of the velocity curve, we subtract the overall streaming motion of the tails, by fitting a 5th order cubic spline (using IRAF’s `curfit` task) to all velocity points. We then extract individual regions from the residual velocity field (see lower part of Fig. 3).

In order to quantify the remaining apparent velocity gradients, we tried to fit a linear relation to all velocity gradients within the spatial extent of the knots. The results are given in Table 1, together with the error given by the fit procedure, the maximum velocity difference ΔV_{max} , and the angular extent of the fitted gradient. The fits seem to be a good first order approximation to the real velocity gradients in most cases, and are shown in the bottom part of Fig. 3. Seven knots show velocity amplitudes that are significant, with errors below 50%. They reach 340 km s^{-1} for object ‘a’. For several knots the gradient is also clearly resolved, i.e. it is observed to extend more than twice the seeing of $1''$.

4. Discussion and Conclusions

Given the observed significant velocity gradients within seven knots of the tails of AM 1353–272 A, we discuss several possibilities of the origin of this specific velocity distribution.

Instrumental errors can be excluded as a cause of these gradients. The velocity profiles observed over very small angular sizes (a few arcseconds) cannot be explained with flexures or distortions of the instrument. The wavelength calibration has been carried out and checked with the procedure described in Sect. 2. As a result, any relative in-

strumental effects within a given slit should be below 1 km s^{-1} .

The apparent gradients could result from projection effects. As the angular size probed is only about 2 to 4 times the seeing, several smaller, physically unrelated knots might appear blended into one larger clump, mimicking the gradient we observe. It seems improbable, however, that this should be the case for many knots. Besides the two well determined tidal tails, there is no indication of complex tidal structures in this system. It is therefore quite unlikely that tidal debris outside the well-defined tails is observed in projection close to so many tidal knots.

Projection effects within a single tail are possible. First, the tails may have some depth along the line of sight, as can be seen in dynamical models of interactions starting with the idea of Toomre & Toomre (1972) to view tails as two-dimensional ribbons. Second, the very tip of the southern tail could indeed be bent. Its three-dimensional shape might partly account for the exceptionally large velocity gradient observed towards condensation ‘a’. An example of a projection by such a bend near the end of a tail is discussed by Hibbard et al. (2001) for the tail of the Antennae galaxies (NGC 4038/39). There, the total H I column density and the velocity dispersion along the line of sight mimic a massive condensation of matter. In their high-resolution H I data, they find two gas concentrations at different velocities, which have only about a tenth of the originally estimated mass. The amplitude $\Delta V_{\text{max}} = 340 \text{ km s}^{-1}$ within knot ‘a’ (compared to $\Delta V_{\text{max}} \sim 50 \dots 100 \text{ km s}^{-1}$ in the Antennae region) makes it seem unlikely to be caused by projection alone. The overall velocity field towards the end of the southern tail is decreasing. If the tail was bent backwards to the center, one would expect this trend to continue. Knots projected from this bent part of the tail should then have even lower velocity than ‘a’. Such velocities are not observed. Projection effects by a bent tail for other knots apart from ‘a’ are implausible.

Velocity gradients could, in principle, be caused by gaseous outflows where one side of an expanding shell is blocked by dust. This would require significant amounts of extinction within the knots, while we find only very moderate absorption ($A_B \lesssim 1.0 \text{ mag}$ including galactic $A_B = 0.26 \text{ mag}$,

Table 1: Velocity gradients within the knots.

ID ^a	ΔV_{\max}^b [km s ⁻¹]	error	extent ^c ["], [kpc]
a	+343	5%	3''0, 2.3
a-to-b ^d	+94	72%	2''0, 1.5
b	+87	21%	2''6, 2.0
c	+34	40%	3''2, 2.5
d	+93	10%	4''2, 2.9
e	-73	65%	2''4, 1.4
f	low S/N
g	+15	170%	4''6, 3.2
k	-50	31%	2''2, 1.7
l	-24	24%	2''6, 2.0
m	-43	19%	3''4, 2.6

^aKnots with significant amplitude of velocity gradient are marked in boldface.

^bGradients with positive sign have the highest velocity towards the north of the system.

^cThe seeing of 1'' at the distance of AM 1353–272 A corresponds to ~ 800 pc.

^dWe designate the region $\pm 1''$ around $+45''.8$ distance from the nucleus as a-to-b.

estimated from Balmer line ratios). Additionally, an outflow would also imply line-broadening. There is no indication of broad lines here, as the FWHM of the H β line is the same as the spectral resolution. It is very unlikely that the gradients are caused by outflows.

Rotation of bound objects could also create this kind of velocity gradients. From the irregular optical appearance and the location of the knots within tidal tails, it is unlikely that the stars in the potential of a knot have stable orbits. True Keplerian motion will not apply here, and it would then be premature to interpret the observed kinematics in terms of “rotation”. Mass estimates from the Virial theorem would strongly overestimate the real mass contained within the knots⁴.

Instead, we may be witnessing the formation of bound objects in the tidal tails which are not yet virialized. The velocity gradients also seem to be specifically oriented in the sense that the higher velocity end of each knot points towards the center of AM 1353–272 A. A possible cause could be the rotational direction of progenitor disk before the interaction. The presence of the companion

galaxy ‘B’ near the southwestern tidal tail could also amplify motions in the tails, to create a “spin” in these knots in one direction. This would also explain the higher velocity amplitudes within the knots in the southwestern tail close to the companion.

The idea of Tidal Dwarf Galaxies (TDGs) — dwarf galaxies that are born as condensations in tidal tails — has been discussed in recent years by several authors (Barnes & Hernquist 1992; Hibbard & Mihos 1995; Duc et al. 1997), both theoretically and observationally. Duc et al. (2000) proposed a first definition of the term TDG as a self-gravitating object of dwarf galaxy mass formed from tidal material (see also Weillbacher & Duc 2001). While we are hampered by the spatial resolution and cannot give the ultimate proof of the velocity gradients as motion of tidal material beginning to get bound into knots, it seems that we are witnessing the formation of TDGs in the tails of AM 1353–272 A, for the first time for multiple objects along both tails of the same interacting galaxy.

Forthcoming instruments for high-resolution spectroscopy on 8m-class telescopes, e.g. integral field instruments, will enable us to confirm the velocity gradients and further investigate their origin. Coupled with the high spatial resolution of adaptive optics these instruments will be very

⁴If caused by Keplerian rotation alone, the rotational velocity of knot ‘a’ would be of the same order as those of giant spiral galaxies, which is unrealistic for an object with $M_B = -13.7$ mag.

useful tools to analyze the unique properties of the knots seen in these tidal tails. To fully understand the geometry and interaction parameters causing this first series of possibly genuine Tidal Dwarf Galaxies and to complement the observations, detailed dynamical N-body+SPH modeling of the collision will be necessary.

We thank I. Appenzeller for help with the proposal and data retrieval and our anonymous referee for a friendly and helpful report. PMW is partly supported by DFG grant FR 916/6-2.

REFERENCES

- Barnes, J. & Hernquist, L. 1992, *Nature*, 360, 715
- Duc, P.-A., Brinks, E., Springel, V., et al. 2000, *AJ*, 120, 1238
- Duc, P.-A., Brinks, E., Wink, J., & Mirabel, I. 1997, *A&A*, 326, 537
- Hibbard, J. & Mihos, J. 1995, *AJ*, 110, 140
- Hibbard, J. E., van der Hulst, J. M., Barnes, J. E., & Rich, R. M. 2001, *AJ*, 122, 2969
- Springel, V. & White, S. D. M. 1999, *MNRAS*, 307, 162
- Toomre, A. & Toomre, J. 1972, *ApJ*, 178, 623
- Weilbacher, P. & Duc, P.-A. 2001, in *Dwarf Galaxies and their Environment*, ed. K. de Boer, R.-J. Dettmar, & U. Klein, 269–272
- Weilbacher, P. M., Duc, P.-A., & Fritze-v. Alvensleben, U. 2002, *A&A*, submitted
- Weilbacher, P. M., Duc, P.-A., Fritze-v. Alvensleben, U., Martin, P., & Fricke, K. J. 2000, *A&A*, 358, 819